Unraveling the role of Mo/Ni synergy in β-$Ni(OH)_2$ for high-performance urea oxidation catalysis

Hsiao-Chien Chen,*[a,b,c] Abdul Shabir,[a,] Kun-Hua Tu[c]

[a]*Dual Master Program in Nano-Electronic Engineering and Design, Chang Gung University, Taoyuan 33302, Taiwan.*
[b]*Center for Sustainability and Energy Technologies, Chang Gung University, Taoyuan 33302, Taiwan*
[c]*Kidney Research Center, Department of Nephrology, Chang Gung Memorial Hospital, Linkou, Taoyuan 33305, Taiwan*
[d]*Center for Reliability Science and Technologies, Chang Gung University, Taoyuan 33302, Taiwan*

*Corresponding author:
E-mail addresses: hc_chen@mail.cgu.edu.tw

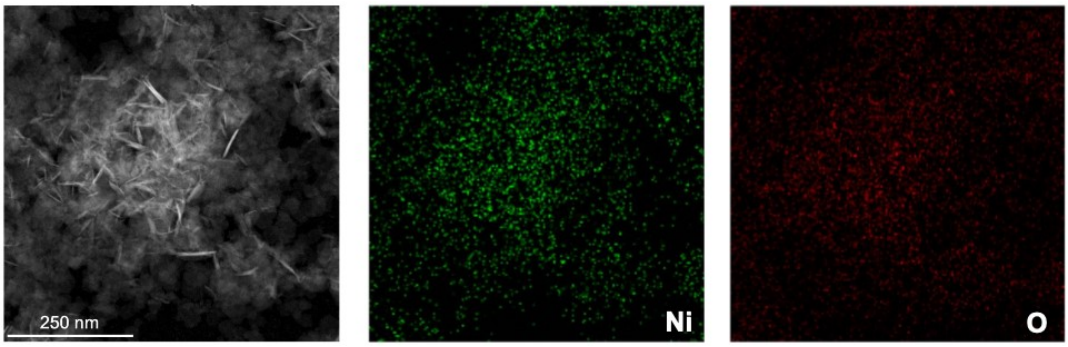

Figure S1. HAADF-STEM-EDS elemental mapping of β-$Ni(OH)_2$.

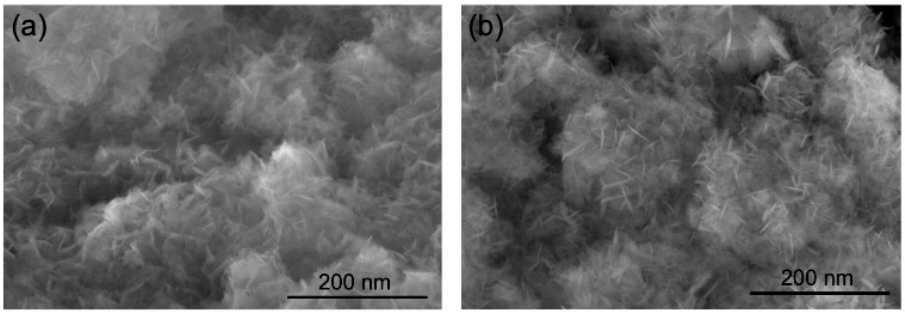

Figure S2. SEM images of (a) β-$Ni(OH)_2$ and (b) Mo/β-$Ni(OH)_2$.

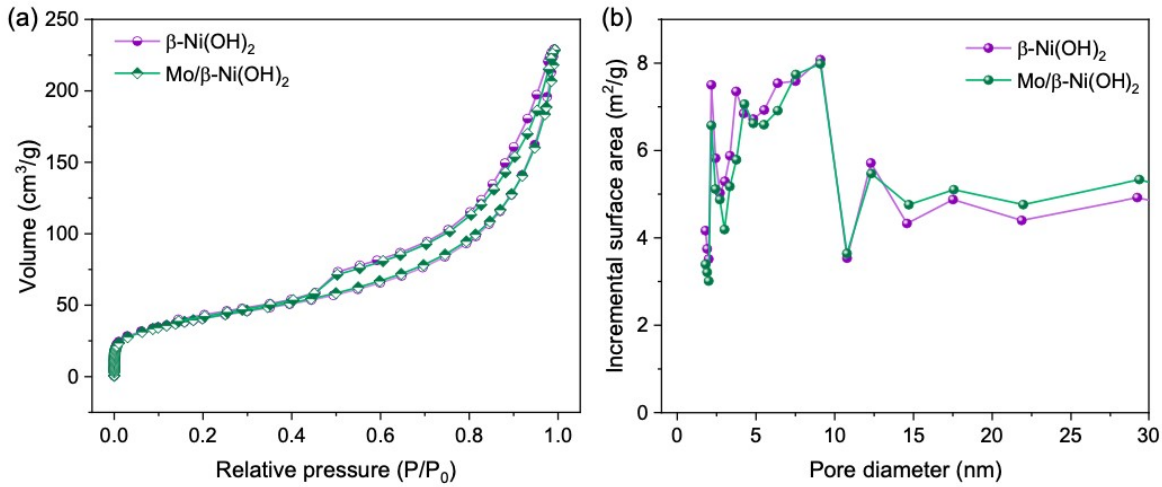

Figure S3. (a) BET plots and (b) BJH plots of β-$Ni(OH)_2$ and Mo/β-$Ni(OH)_2$.

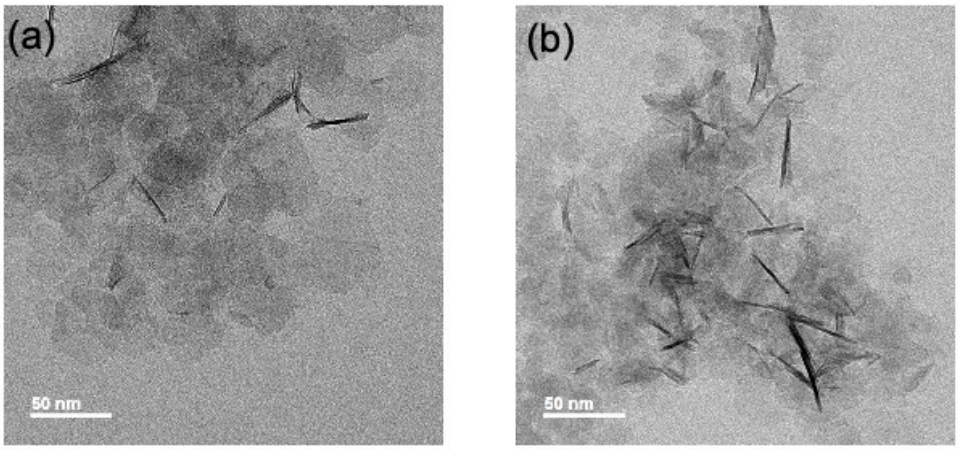

Figure S4. TEM images of (a) β-$Ni(OH)_2$ and (b) Mo/β-$Ni(OH)_2$.

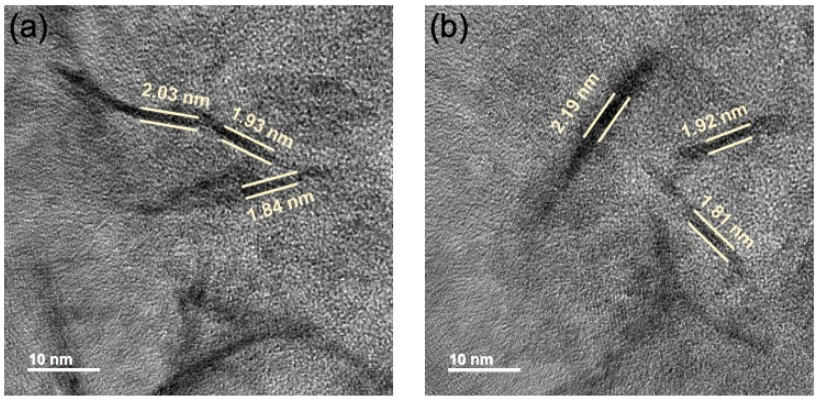

Figure S5. TEM images of (a) β-$Ni(OH)_2$ and (b) Mo/β-$Ni(OH)_2$.

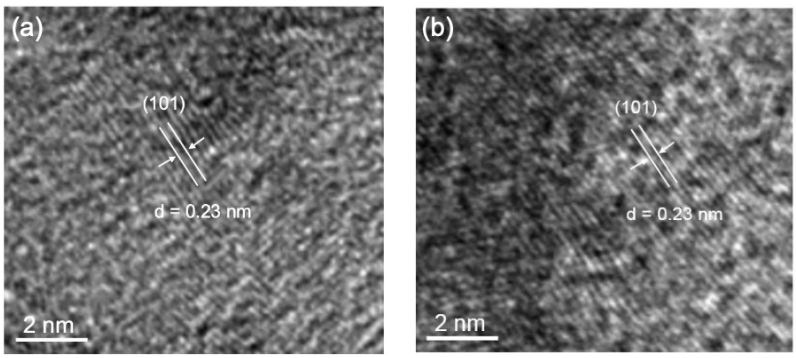

Figure S6. HRTEM images of (a) β-$Ni(OH)_2$ and (b) Mo/β-$Ni(OH)_2$.

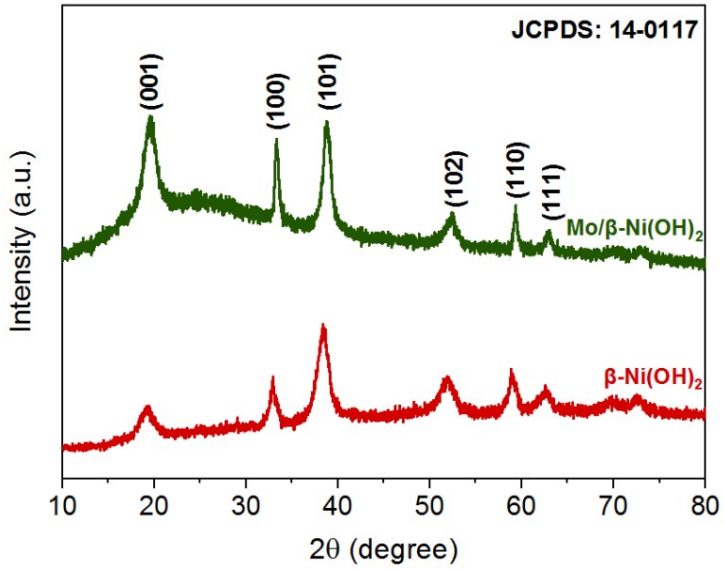

Figure S7. XRD patterns of (a) β-$Ni(OH)_2$ and (b) Mo/β-$Ni(OH)_2$.

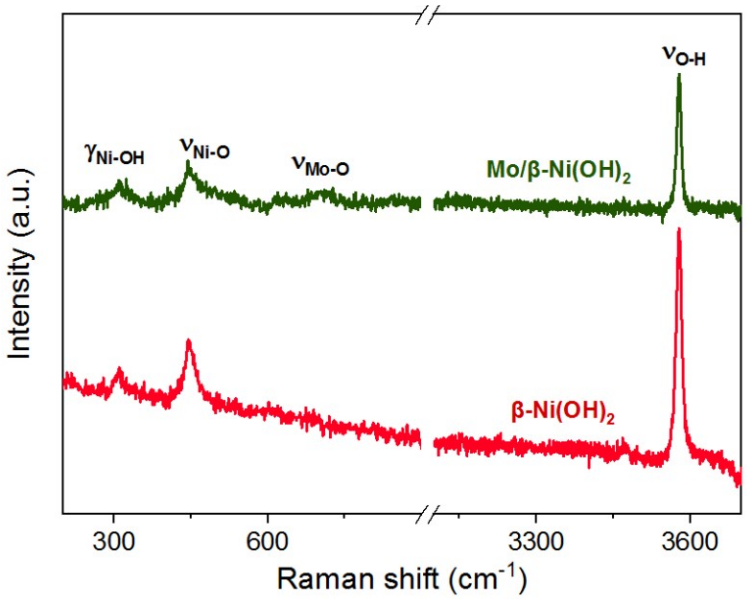

Figure S8. Raman spectra of (a) β-$Ni(OH)_2$ and (b) Mo/β-$Ni(OH)_2$.

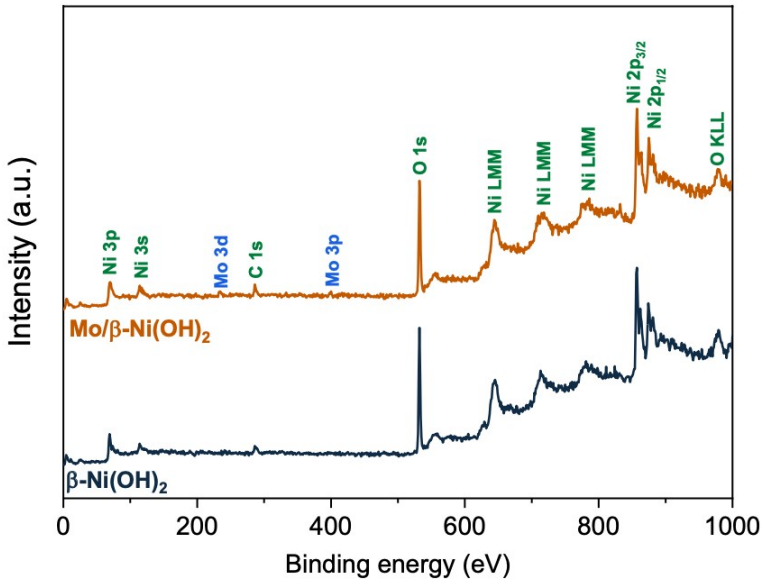

Figure S9. XPS survey spectrum of β-$Ni(OH)_2$ and Mo/β-$Ni(OH)_2$.

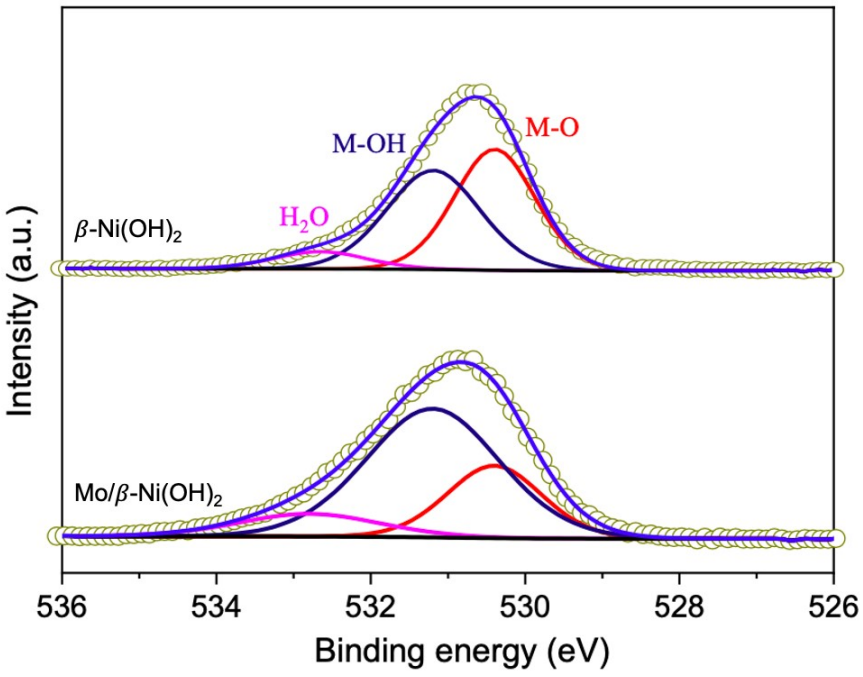

Figure S10. High-resolution XPS spectra of O 1*s*.

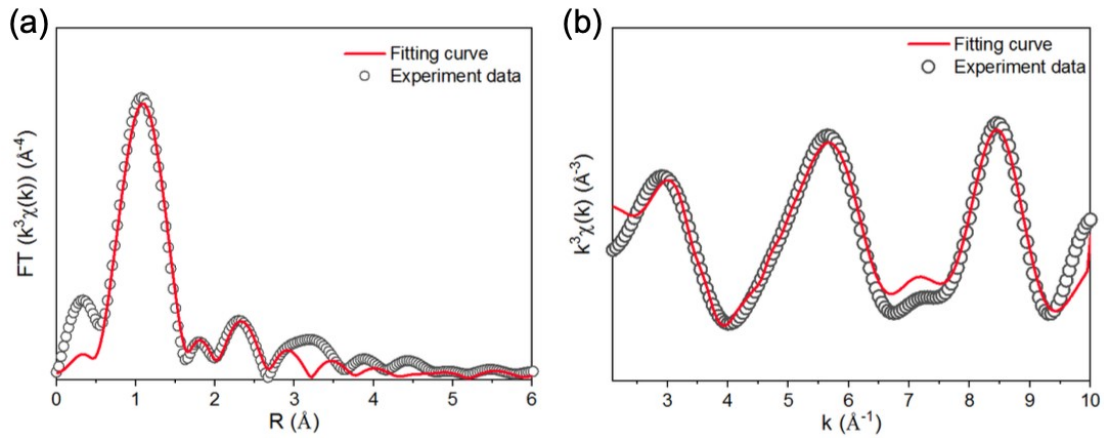

Figure S11. (a) The fitting curve of EXAFS spectrum of Mo for Mo/β-Ni(OH)$_2$ and (b) its k space fitting curve.

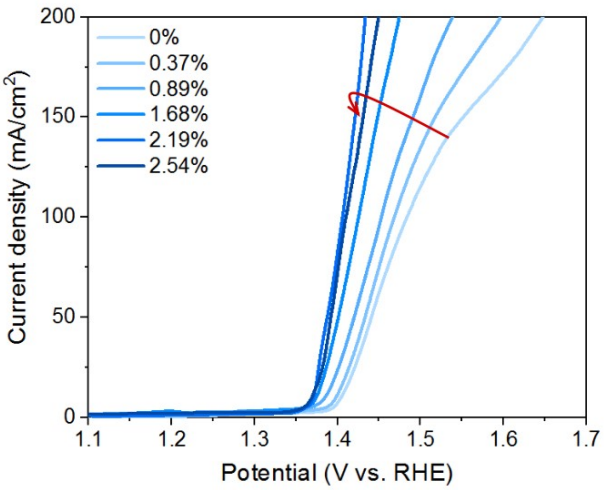

Figure S12. UOR polarization curves of Mo/β-Ni(OH)$_2$ with different Mo weight contents.

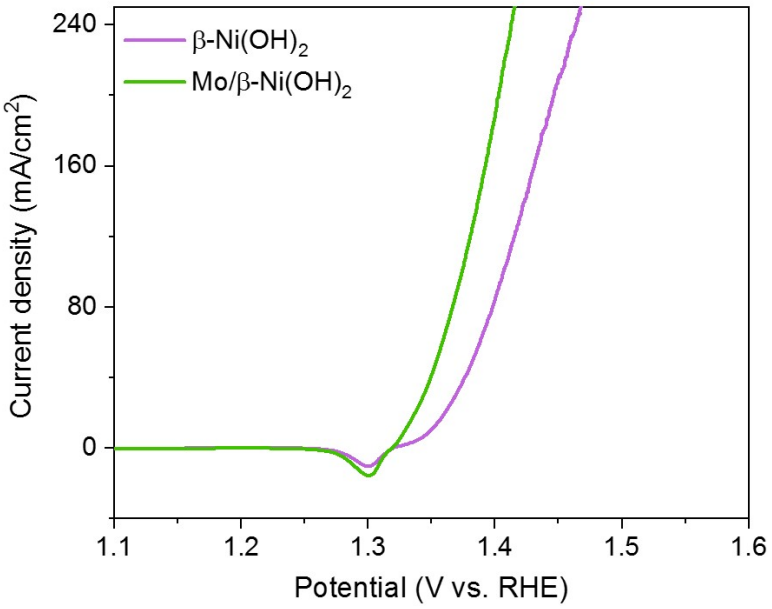

Figure S13. Polarization curves for UOR through negative scan.

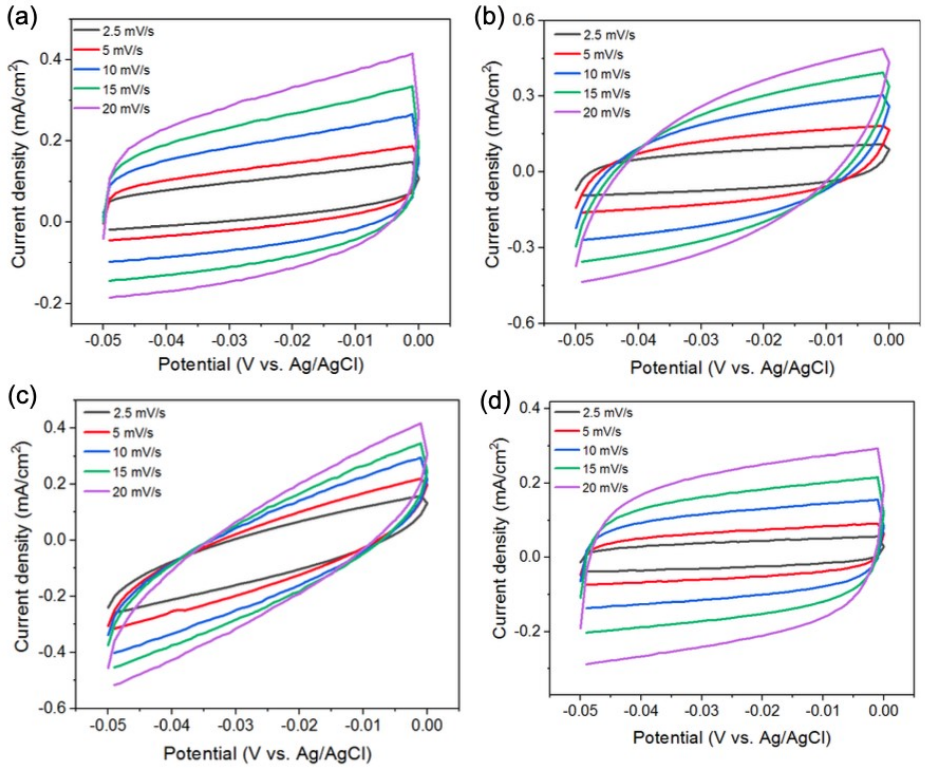

Figure S14. Cyclic voltammetry (CV) curves at different scan rates in the non-Faradaic capacitance current range for (a) β-$Ni(OH)_2$, (b) MoO_3/β-$Ni(OH)_2$, (c) MoO_3 and (d) Mo/β-$Ni(OH)_2$.

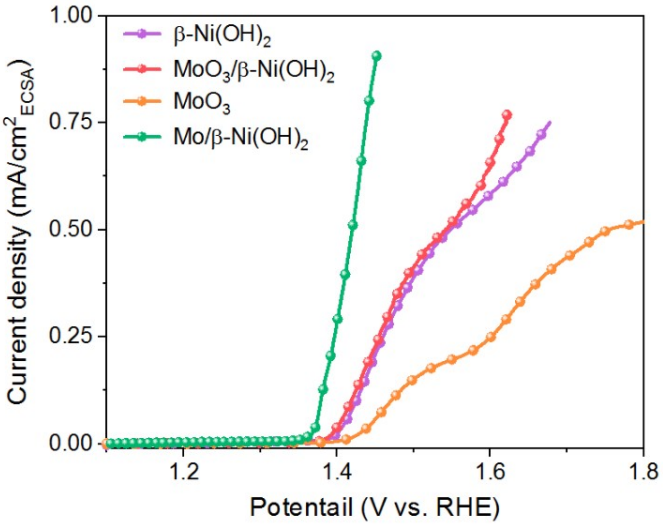

Figure S15. UOR polarization curves of β-$Ni(OH)_2$, MoO_3/β-$Ni(OH)_2$, MoO_3 and Mo/β-$Ni(OH)_2$ after normalized by ECSA.

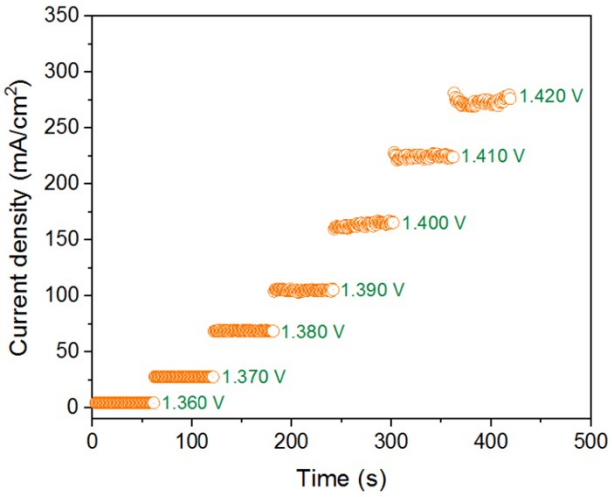

Figure S16. Multi-step chronopotentiometric test of Mo/β-$Ni(OH)_2$ at different potentials.

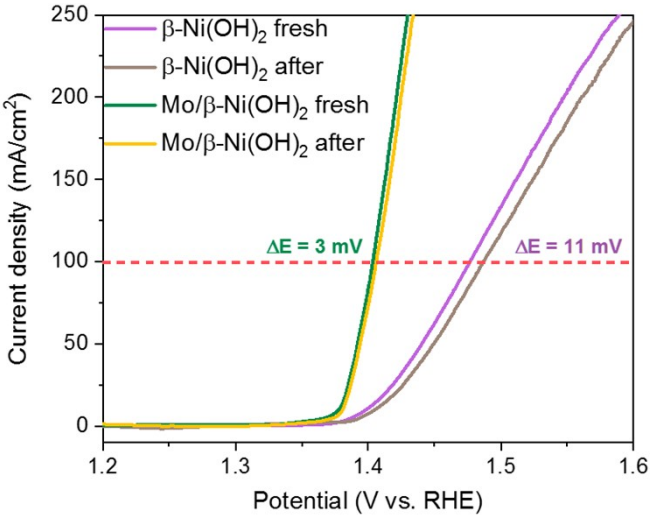

Fig. S17. The UOR polarization curves before and after prolonged UOR testing.

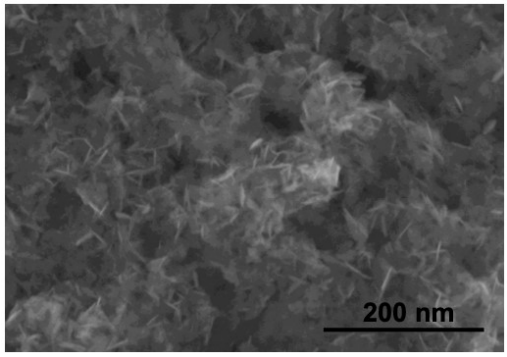

Figure S18. SEM image of β-Ni(OH)$_2$ after 40 h of stability test.

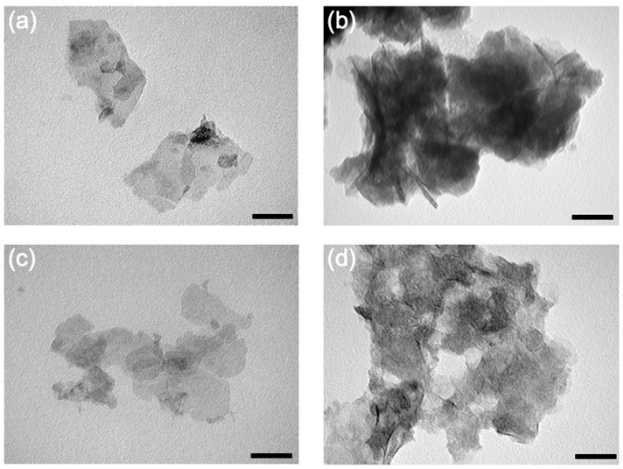

Fig. S19. TEM images of (a, c) β-Ni(OH)$_2$ and (b, d) Mo/β-Ni(OH)$_2$ acquired before and after prolonged UOR testing. The scale bar in each image corresponds to 50 nm.

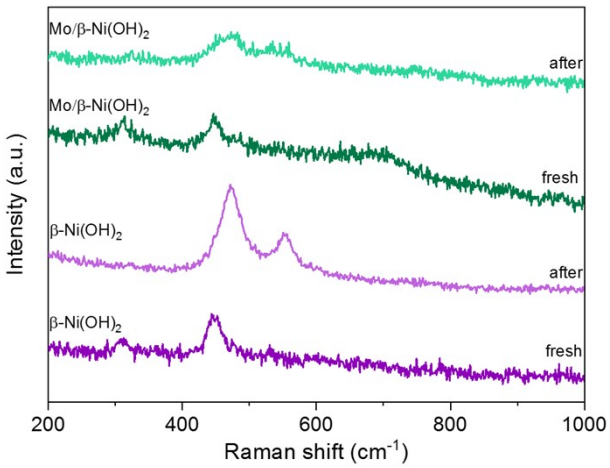

Figure S20. Raman spectra of β-$Ni(OH)_2$ and Mo/β-$Ni(OH)_2$ acquired before (at OCV state) and after prolonged UOR testing.

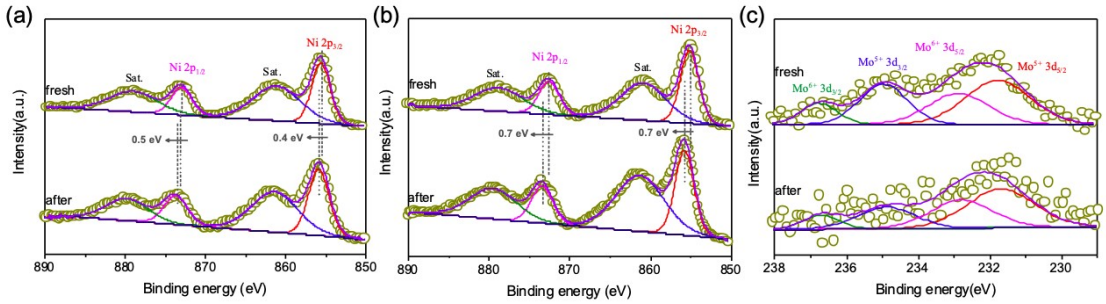

Figure S21. High-resolution XPS spectra of (a) Ni 2*p* in β-$Ni(OH)_2$, (b) Ni 2*p* and (c) Mo 3*d*. in Mo/β-$Ni(OH)_2$ before and after prolonged UOR testing.

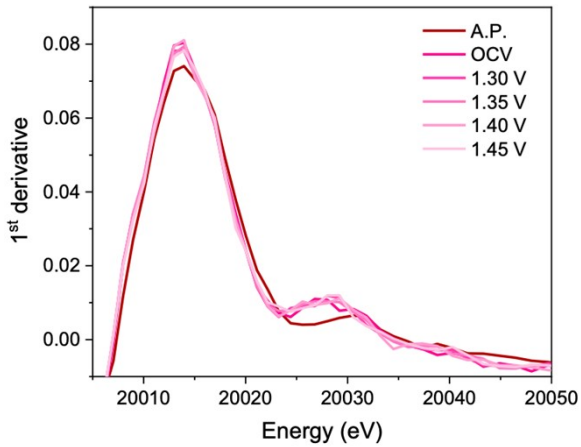

Figure S22. The dynamic 1st derivative spectra of Mo K-edge XANES.

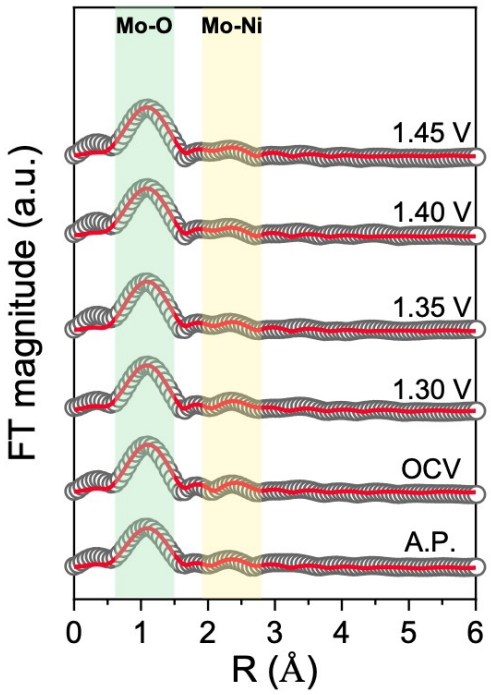

Figure S23. *In situ* Mo K-edge EXAFS fitting curves in R space of Mo/β-Ni(OH)$_2$.

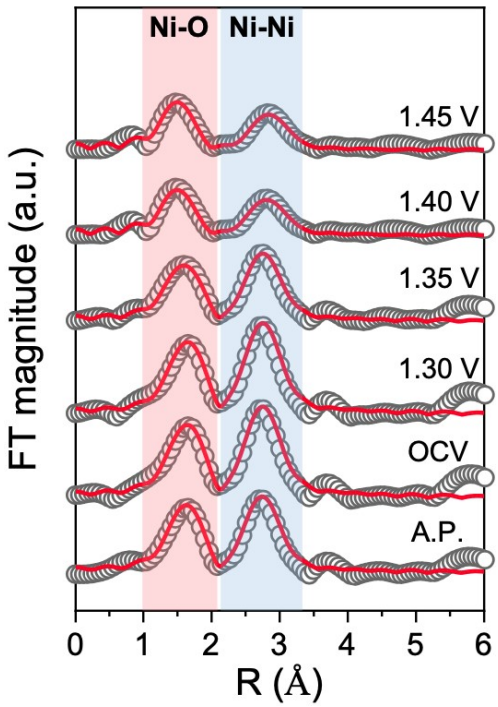

Figure S24. *In situ* Ni K-edge EXAFS fitting curves in R space of β-Ni(OH)$_2$.

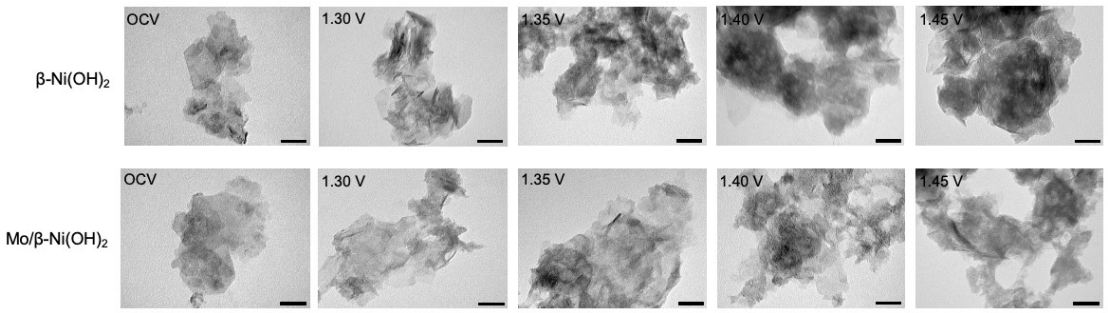

Figure S25. *Ex situ* TEM images of β-$Ni(OH)_2$ and Mo/β-$Ni(OH)_2$ samples collected after electrochemical polarization at different anodic potentials (OCV to 1.45 V). The scale bar in each image corresponds to 50 nm.

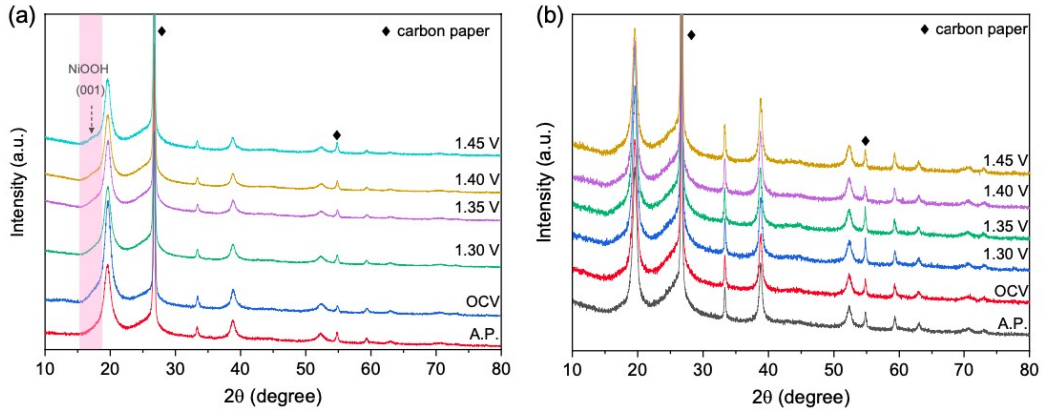

Figure S26. *Ex situ* XRD of (a) β-$Ni(OH)_2$ and (b) Mo/β-$Ni(OH)_2$ from the A.P. state to 1.45 V.

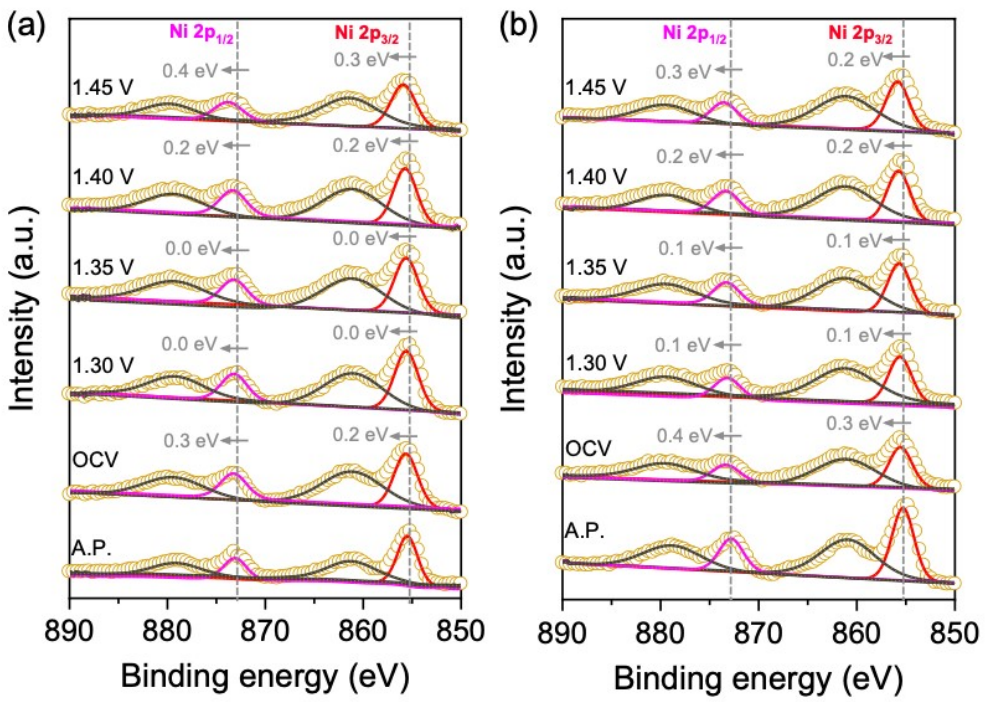

Figure S27. *Ex situ* Ni 2*p* XPS of (a) β-Ni(OH)$_2$ and (b) Mo/β-Ni(OH)$_2$ from the A.P. to 1.45 V.

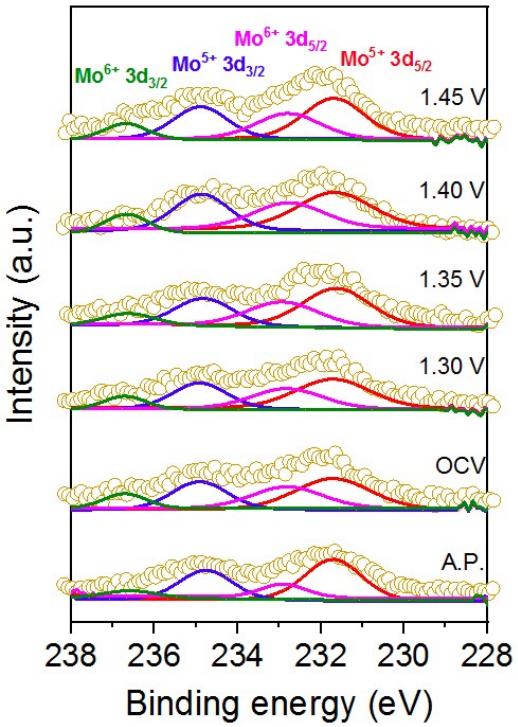

Figure S28. *Ex situ* Mo 3*d* XPS of Mo/β-Ni(OH)$_2$ from the A.P. to 1.45 V.

Table S1. ICP-OES analysis of Mo_x/β-$Ni(OH)_2$.

Mo_x/β-$Ni(OH)_2$ ($0 \leq x \leq 100$, mass ratio, %)	Precursor solution (mg)		Metallic mass ratio (%)	
	β-$Ni(OH)_2$	$MoCl_5$	Ni	Mo
β-$Ni(OH)_2$	50	0	100	0
$Mo_{0.37}$/β-$Ni(OH)_2$	50	1	99.63	0.37
$Mo_{0.89}$/β-$Ni(OH)_2$	50	2	99.11	0.89
$Mo_{1.68}$/β-$Ni(OH)_2$	50	3	98.32	1.68
$Mo_{2.19}$/β-$Ni(OH)_2$	50	4	97.81	2.19
$Mo_{2.54}$/β-$Ni(OH)_2$	50	5	97.46	2.54

Table S2. Structural parameters extracted of Mo/β-$Ni(OH)_2$.

Condition	Path	CN*	R (Å)	dE (eV)	DW ($Å^3$)
Mo/β-$Ni(OH)_2$	Mo-O	3.8 (2)	1.69 (1)	-2.7 (4)	0.0033 (6)
	Mo-Ni	0.9 (2)	2.65 (2)	-5.5 (5)	0.0097 (4)

*CN: coordination number

Table S3. Structural parameters extracted of Mo/β-$Ni(OH)_2$ from *in situ* Mo K-edge EXAFS during UOR.

Condition	Path	CN*	R (Å)	dE (eV)	DW ($Å^3$)
As prepared	Mo-O	3.8 (2)	1.69 (1)	-2.7 (4)	0.0033 (6)
	Mo-Ni	0.9 (2)	2.65 (2)	-5.5 (5)	0.0097 (4)
OCV	Mo-O	3.9 (3)	1.71 (3)	-4.3 (6)	0.0041 (6)
	Mo-Ni	0.9 (2)	2.66 (1)	-4.4 (6)	0.0091 (6)
1.30 V	Mo-O	3.8 (3)	1.70 (3)	-4.8 (6)	0.0039 (7)

1.35 V	Mo-Ni	0.8 (3)	2.67 (2)	-3.9 (5)	0.0095 (6)
	Mo-O	3.9 (2)	1.71 (2)	-4.2 (6)	0.0044 (7)
	Mo-Ni	0.9 (3)	2.66 (3)	-3.5 (6)	0.0102 (6)
1.40 V	Mo-O	4.0 (2)	1.71 (3)	-4.9 (5)	0.0040 (7)
	Mo-Ni	1.0 (2)	2.65 (2)	-4.4 (6)	0.0105 (7)
1.45 V	Mo-O	3.9 (1)	1.71 (3)	-4.2 (6)	0.0037 (6)
	Mo-Ni	0.9 (2)	2.67 (3)	-4.5 (6)	0.0099 (7)

*CN: coordination number

Table S4. Structural parameters extracted of Mo/β-$Ni(OH)_2$ from *in situ* Ni K-edge EXAFS during UOR.

Condition	Path	CN*	R (Å)	dE (eV)	DW ($Å^3$)
As prepared	Ni-O	5.7 (3)	2.03 (2)	-2.4 (4)	0.0065 (6)
	Ni-Ni	5.6 (3)	3.10 (3)	3.8 (6)	0.0068 (5)
OCV	Ni-O	5.8 (2)	2.03 (2)	-3.4 (5)	0.0057 (6)
	Ni-Ni	5.8 (3)	3.10 (4)	4.2 (6)	0.0067 (4)
1.30 V	Ni-O	5.7 (2)	2.03 (3)	-3.4 (5)	0.0045 (7)
	Ni-Ni	5.8 (1)	3.11 (3)	4.1 (6)	0.0066 (4)
1.35 V	Ni-O	5.6 (3)	2.03 (3)	-2.4 (6)	0.0057 (6)
	Ni-Ni	5.7 (1)	3.11 (4)	4.4 (6)	0.0064 (4)
1.40 V	Ni-O	5.5 (3)	2.02 (4)	-4.1 (5)	0.0059 (6)
	Ni-Ni	5.4 (3)	3.13 (4)	5.1 (6)	0.0077 (6)
1.45 V	Ni-O	5.5 (4)	1.98 (4)	-3.6 (5)	0.0066 (6)
	Ni-Ni	5.3 (3)	3.16 (3)	5.4 (5)	0.0080 (5)

*CN: coordination number

Table S5. Structural parameters extracted of β-$Ni(OH)_2$ from *in situ* Ni K-edge EXAFS during UOR.

Condition	Path	CN*	R (Å)	dE (eV)	DW ($Å^3$)
As prepared	Ni-O	5.6 (2)	2.02 (3)	-1.5 (4)	0.0058 (7)
	Ni-Ni	5.7 (1)	3.13 (5)	3.7 (5)	0.0061 (6)
OCV	Ni-O	5.8 (2)	2.03 (3)	-0.9 (5)	0.0062 (8)
	Ni-Ni	5.9 (1)	3.13 (3)	3.8 (5)	0.0052 (6)
1.30 V	Ni-O	5.8 (2)	2.03 (4)	-0.6 (4)	0.0062 (7)
	Ni-Ni	5.9 (2)	3.13 (2)	3.9 (5)	0.0053 (5)
1.35 V	Ni-O	5.7 (3)	2.01 (3)	-2.5 (5)	0.0072 (6)
	Ni-Ni	5.8 (2)	3.16 (4)	4.5 (3)	0.0061 (5)
1.40 V	Ni-O	5.5 (3)	1.95 (4)	-9.1 (4)	0.0050 (6)
	Ni-Ni	5.7 (4)	3.22 (4)	5.0 (5)	0.0079 (4)
1.45 V	Ni-O	5.6 (4)	1.90 (4)	-9.2 (6)	0.0052 (7)
	Ni-Ni	5.8 (4)	3.27 (3)	4.9 (5)	0.0079 (5)

*CN: coordination number